Souphanouvong University Journal of Multidisciplinary Research and Development
2026, Vol. 12, [Fast Track], 275-284
https://doi.org/10.69692/SUJMRD12(Fast track)275

Hybrid Solar–Electric Kiln for Sustainable Timber Drying: Temperature Stabilization, Equilibrium Moisture Conditions, and Grid-Energy Savings Under a Temperate Winter Climate

Khamtan Phonetip*, Benoit Belleville[a], Leon Chan[b]

[a]*School of Agriculture, Food, and Ecosystem Sciences, Faculty of Science, The University of Melbourne, 500 Yarra Boulevard, Richmond, Victoria 3121, Australia. Email: benoit.belleville@unimelb.edu.au*
[b]*Department of Mechanical Engineering, Faculty of Engineering and Information Technology, University of Melbourne, Melbourne, VIC 3010, Australia. Email: lzhchan@unimelb.edu.au*

Correspondence:
Khamtan Phonetip, Faculty of Forest Science, National University of Laos, Vientiane Capital, Laos. Tel: +856-21 770097, Fax:+856-21 770294, Email: k.phonetip@nuol.edu.la

Article Info:
Submitted: June 02, 2026
Revised: June 19, 2026
Accepted: June 30, 2026

Abstract

Solar kilns offer a low-operational cost alternative to conventional timber drying but suffer from weather-dependent temperature instability that limits industrial uptake. This study evaluated a 0.94 m³ hybrid solar–electric kiln prototype that combines passive solar gain with a thermostatically controlled 2 kW electric booster, with the aim of quantifying its temperature stabilisation, equilibrium moisture conditions, and grid-energy contribution under Melbourne winter conditions in Australia. Three solar-only and three hybrid trials (09:00–16:00, 50 °C setpoint) were conducted in July-August 2025 at the Burnley Campus, Richmond, Victoria (37.83 °S, 145.02 °E). Ambient temperature, relative humidity, and global horizontal irradiance were obtained from CERRA reanalysis and CAMS at five-minute resolution. Without auxiliary heat, the kiln temperature rose approximately10 °C above ambient on overcast days and reached the 50 °C setpoint only briefly on the sunniest day, fluctuating with the insolation. With auxiliary heating, the kiln reached the 50 °C setpoint within 15–30 min and was maintained at 50 ± 1 °C, approximately 25 % above the typical solar-only midday peak of ~40 °C, and the kiln-air equilibrium moisture content (EMC) decreased from ~6 % to ~3 %. A linear regression of kiln temperature on ambient temperature, ambient relative humidity, and irradiance achieved $R^2 = 0.70$ on the training data. The hybrid system displaced 25–79 % of the heating energy that would otherwise have been drawn from the grid, expressed as a solar contribution fraction (SCF) relative to continuous heater operation. These results indicate that low-cost hybrid solar–electric kilns can deliver stable thermodynamic drying conditions while substantially reducing grid-energy demand, even in temperate winter climates.

Keywords: Solar kiln; hybrid drying; equilibrium moisture content; solar contribution fraction; reanalysis data; empirical model

1. Introduction

Solar-assisted kilns have gained attention as a pathway to reduce energy use and emissions by harnessing renewable solar radiation to heat lumber, offering cost and environmental benefits over gas-fired or purely electric kilns. Experimental work published previously demonstrated that a modified passive solar kiln could dry hardwood to commercial standards in under a month, confirming its feasibility as a viable alternative to conventional fuel-based kilns (De Vore et al., 1999) and developed early heat and mass transfer simulations to optimize solar-kiln design (Helwa et al., 2004; H. A. Khater et al., 2004). Solar kilns without auxiliary heat are weather-dependent, leading to slower drying rates and fluctuating temperatures and humidity (Phonetip et al., 2022). Recent comparative studies of solar dryers with thermal storage deliver steadier drying and higher efficiency than plain solar units, making hybridization the most effective solution to overcome solar intermittency (Monesh et al., 2024).

Recent advances in solar-assisted kilns integrate automated control and auxiliary heating, enabling industrial-scale drying with lower costs and improved timber quality (Bux et al., 2001). A solar kiln with modest firewood backup, a solar kiln can be thermally effective and economically and environmentally attractive, but its performance is strongly constrained by the local climate (Simo-Tagne & Ndi-Azese, 2021). Although focused on agricultural products, the review by Udomkun et al (2020) clearly showed that solar-only dryers suffer from intermittency, and several authors have recommended hybrid or solar-plus-storage configurations to maintain target drying conditions (Simo-Tagne et al., 2020). Consistent with this, Khouya (2020) found that integrating heat regeneration and thermal energy storage into a solar hardwood kiln reduced total energy consumption by roughly 50% versus a conventional kiln, primarily by smoothing short-term solar variability. A subsequent energy analysis of a combined solar wood-drying system showed that supplementing solar energy with an auxiliary heat-pump unit during periods of low irradiance improved temperature control while still reducing specific energy consumption relative to a conventional dryer (H. A. Khater et al., 2004). Closer to the configuration tested here, Lamrani et al. (2020) modelled a hybrid solar–electrical wood dryer integrated with a latent-heat thermal-energy-storage system, and Lamrani et al. (2021) subsequently reported that combining a photovoltaic/thermal collector with a heat-recovery unit reduced annual energy consumption of conventional wood dryers by up to 67.5 % in hot climates and 49.5 % in cold climates. An experimental and techno-economic study by Thomasson et al.(2024) reported that a solar-assisted heat-pump biomass dryer in Finland increased the drying rate more than threefold (33.0 vs. 9.0 kg h^{-1}) compared to a conventional dryer, though this improvement came with a 45% rise in specific electricity consumption, underscoring the trade-offs inherent in hybrid drying systems. A recent review confirmed that hybrid solar kilns, including solar–electric and solar–biomass configurations and those incorporating thermal storage, consistently achieve more stable temperatures, shorter drying times, and better product quality than purely solar systems (Kong et al., 2024).

Early evidence using local climate inputs showed that solar-assisted schedules can be planned and optimised for specific sites. For example, Phonetip et al.(2018) simulated a solar-kiln schedule for tropical areas using a conventional kiln, demonstrating that local irradiance can be used to anticipate kiln behaviour prior to construction. Khouya (2020) coupled a heat pump with a photovoltaic/thermal (PV/T) collector, reporting higher efficiency and reduced grid dependence relative to non-hybrid baselines. In *Drying Technology*, a thermal recharge–discharge model derived from conventional-kiln measurements predicted internal solar-kiln temperature to within ± 2 °C and produced *Eucalyptus delegatensis* boards dried to 12 % MC in 87 days at an average rate of 0.2 % MC day^{-1}(Phonetip, Brodie, et al., 2019). A companion study showed that intermittent solar-style schedules (45 °C / 60 % RH heating, 80–90 % RH non-heating) gave AS/NZS 4787:2001 class-A quality on the same species,(Phonetip, Ozarska, et al., 2019) establishing that solar-driven cyclic regimes can match conventional-kiln quality. Ferrari et al.(2024) field-validated a pilot solar-plus-biomass indirect kiln in which an auxiliary biomass furnace accelerated drying from ≈0.4 % MC day^{-1} (solar alone) to ≈1.4 % MC day^{-1} and lowered final moisture content relative to open-air drying. From an end-use perspective, solar-plus-grid hybrids are particularly attractive in regions where the grid is largely renewable or where local biomass supply chains are constrained.

Further comparative work underscores how collector and system choices affect outcomes. Chtioui and Khouya (2024) showed that PV/T and double-pass solar-air collectors improve temperature profiles and throughput across climates, supporting the case for hybridisation. Hybridisation, often complemented by thermal storage, delivers the largest gains in energy efficiency and process reliability compared to solar-only drying (G. Khater et al., 2024). Lamrani et al.(2023) in a one-year simulation of a solar wood dryer, found that chamber air temperature varied widely with the weather and that maintaining a high setpoint was challenging without auxiliary heat.

Crucially, kiln-temperature stability is improved when hybrid solar kilns are actively managed. Weather-aware, sensor-driven control of auxiliary heat and airflow can shorten drying time by up to 35 % while stabilising temperature and relative humidity, thereby improving both energy performance and product quality(Chtioui & Khouya, 2024; Ferrari et al., 2024; Khouya, 2020). Recent advances in this direction include a model-based optimisation framework that couples PV/T thermal output to harmonic-function drying schedules to absorb renewable-energy fluctuations during beech-board drying (Stéphan et al., 2025) and an air-energy-assisted solar system tested in north-east China that achieved a 50.7 % electrical-energy improvement when the auxiliary heat was applied intermittently rather than continuously(Chi et al., 2022). Both studies emphasized that the value of hybridisation lies as much in the control logic as in the auxiliary hardware itself.

Despite this growing body of work, three gaps remain. First, almost all reported hybrid solar kilns are pilot or industrial-scale; there is little evidence on whether the same approach is viable at sub-cubic-metre scale relevant to smallholders and developing-country sawmills. Second, kiln-temperature regressions in the literature typically rely on on-site instrumentation, whereas freely available reanalysis products (e.g., Copernicus CERRA, CAMS) could in principle support siting decisions before any sensor is installed. Third, the grid-energy contribution of a simple thermostatically controlled hybrid has not been quantified for a temperate winter climate, which is a conservative test case relative to the tropical sites where such systems are most likely to be deployed. For context, Ferrari et al.(2024) reported specific energy costs of approximately USD 0.009 kWh^{-1} for biomass furnace heat, USD 0.05 kWh^{-1} for solar-thermal collectors, and USD 0.14 kWh^{-1} for photovoltaic electricity in their case study; these values are strongly on site conditions and system scale.

Accordingly, the objectives of this study were to (i) characterise the kiln-temperature and kiln-air EMC behaviour of a 0.94 m^3 hybrid solar–electric kiln prototype under solar-only and hybrid (thermostatically controlled 2 kW booster) operation; (ii) develop an empirical regression that estimates kiln temperature from publicly available reanalysis-based ambient temperature, relative humidity, and global horizontal irradiance; and (iii) quantify the fraction of heating energy displaced by solar gain across days of contrasting cloud cover, expressed as a solar contribution fraction rather than as a saving against a continuous-heating baseline. The work is positioned as a proof-of-concept that explicitly does not include a wood load; the implications for actual timber drying are framed as hypotheses to be tested in subsequent work.

2. Materials and methods

The prototype hybrid solar kiln combined passive solar gain with a thermostatically controlled 2 kW electric booster fan-heater. It was monitored under the cool, damp, and frequently overcast conditions typical of the Melbourne winter in Australia. Kiln-air temperature, ambient temperature, ambient relative humidity, and global horizontal irradiance (GHI) were collected in two operating modes solar-only and solar-plus-auxiliary and used to compare thermal performance, estimate the kiln-air EMC, develop an empirical regression of kiln temperature on ambient conditions, and quantify the solar contribution to heating energy.

2.1 Experimental setup

The prototype was designed and fabricated by the authors and installed at 37.8296 °S, 145.0238 °E (Burnley Campus, Richmond, Victoria, Australia). The roof of the kiln faced north at an angle of 20° from the horizontal plane. The prototype had a chamber volume of 0.94 m^3 (Figure 1). A clear plastic sheet formed the outer transparent envelope (roof and walls); the inner roof layer was a matt-black-painted aluminium sheet acting as the solar absorber, separated from the clear plastic by a 15cm spacing. The aluminium black-sheet had five circulated air inlets (I1–I5) originating from a back wall, each with an area of 180 cm^2 (2x90cm). An evaporated Air vent (10cm diameter), air circulation was provided by two 120 mm PWM-controlled DC axial fan (Delta TFC1212DE, 12 V, free-air rating ~250 CFM at ~5500 rpm) strategically positioned at the middle-top of the kiln. A second STC-1000/STC-3028 controller (220 V) switched a 2kW electric heater fan on and off according to the kiln-temperature setpoint with a controller hysteresis band of ±1 °C. Volumetric flow under installed back-pressure was not directly measured; this is acknowledged as a limitation.

2.2 Data collection and analysis

Six experimental days were conducted between July and August 2025: three solar-only days (heater disabled) and three hybrid days (heater enabled), each running 09:00–16:00 local time. The kiln-air setpoint was 50 °C. The circulation fan ran continuously while the heater cycled on a ± 1 °C hysteresis around the setpoint.

Kiln-air temperature and relative humidity were logged from the STC-3028 controller at 1-minute intervals. Ambient air temperature and relative humidity were obtained from the Copernicus CERRA sub-daily regional reanalysis(Copernicus Climate Change Service, 2025) at the grid point nearest to the site; GHI was obtained from CAMS solar-radiation time series(Copernicus Atmosphere Monitoring Service, 2025) at 5-minute intervals. The choice of reanalysis data was deliberate: it allows the regression model developed to be applied for site-selection purposes before any on-site sensor is deployed.

Kiln-air EMC was estimated from the kiln-air temperature and relative humidity using the Hailwood–Horrobin sorption model in the form recommended by the USDA *Wood Handbook*, (Glass & Zelinka, 2010) which is appropriate for the temperature and RH ranges observed here. Values of EMC below approximately 3 % are reported but are recognised as being at the lower limit of validity of the model and should be interpreted as indicative.

Energy consumption was estimated from the loads (total 2093.6 W), which included the electric heater fan (2000 W) and two blower fans (93.6 W). Heater on-time was logged via the controller relay state. The energy consumption of the fans alone was calculated using Equation (1), and the total nominal energy consumption with the heater also operating using Equation (2). Equation (3) gives the real-time energy use based on logged heater runtime, and Equation (4) defines the solar contribution fraction (SCF) relative to a hypothetical 7-h continuous-heating baseline. SCF should be interpreted as the fraction of the maximum possible heater duty that was offset by solar gain, not as a saving relative to a real conventional kiln, which would itself cycle thermostatically.

$$E_{fans}(t) = P_{fans} \times t \quad (1)$$

where P_{fans} = 93.6 W (two fans, 12 V × 3.9 A × 2); *t* is time in hours; $E_{fans}(t)$ is energy use in Wh.

$$E_{total}(t) = (P_{fans} + P_{heater}) \times t \quad (2)$$

where P_{heater} = 2000 W, giving a total nominal power of 2093.6 W.

$$E_{rt}(t) = (P_{fans} + P_{heater}) \times t_{on} \quad (3)$$

where t_{on} is the cumulative heater on-time over the session.

$$SCF(t) = [E_{total}(t) - E_{rt}(t)] / E_{total}(t) \times 100\ \% \quad (4)$$

3. Results

3.1 Kiln temperature without auxiliary heat

In the solar-only trials (no auxiliary heat), the internal kiln temperature closely followed the diurnal pattern of solar irradiance. Over three days of mostly clear skies with intermittent cloud cover (generally <50 % of the sky), the peak kiln-air temperature reached approximately 40 °C on Day 1 and Day 2, and approximately 52 °C on Day 3 (the day of highest irradiance). Figure 2 shows the kiln temperature profile alongside the ambient air temperature, the 50 °C setpoint, and GHI. In the mornings, the kiln warmed from an ambient of approximately 15 °C as the sun rose. By midday of Day 1 the kiln levelled off at approximately 38–40 °C, 9.6 ± 0.8 °C above ambient (mean ± SD over 11:00–14:00). A similar pattern occurred on Day 2 (peak ~40 °C, 8.9 ± 0.7 °C above ambient). On Day 3, however, intense irradiance in the late morning pushed the kiln temperature rapidly upward, and it briefly exceeded the 50 °C setpoint, reaching a maximum of ~52 °C before noon. This short overshoot occurred under a burst of high irradiance; the vents and natural losses then brought the temperature back down toward 50 °C. Overall, without the heater, the kiln rarely maintained ≥ 50 °C for more than ~3 h, and only on Day 3. The dependence on solar input is evident: mid-session average GHI was approximately 620 W m^{-2} on Day 1,490 W m^{-2} on Day 2 (more cloud), and 890 W m^{-2} on Day 3; only under the highest irradiance did the kiln air briefly reach the target temperature. Throughout the afternoons, as the GHI declined, the kiln temperature also decreased, underscoring the lack of any thermal storage or backup heating in this mode.

3.2 Predicted kiln temperature

A multiple linear regression of 1-min kiln-air temperature on ambient temperature (T_a), ambient relative humidity (RH_a), and GHI was fitted to the three solar-only days ($n \approx$ 1,260 observations after quality control). The training-set coefficient of determination was R^2 = 0.70, indicating that approximately 70 % of the within-session variance in kiln temperature could be explained by simultaneous changes in the three predictors. The very large negative intercept and the apparently high coefficient on T_a reflect strong multicollinearity among T_a, RH_a, and GHI in this small training set; coefficients should therefore be regarded as descriptive of the joint diurnal trajectory rather than as independent partial effects.

3.3 Predicted kiln-temperature model:

$$P_{kt} = -346.701 + 14.067 \times T_a + 2.552 \times RH_a + 3.013 \times GHI \quad (5)$$

where P_{kt} is the predicted kiln temperature (°C), T_a is the ambient temperature (°C), RH_a is the ambient relative humidity (%), and GHI is the instantaneous global horizontal irradiance at the surface (W m^{-2}). The units must match the training data; mixing kWh m^{-2} day^{-1} with W m^{-2} will produce nonsensical predictions.

3.4 Kiln temperature with auxiliary heat

In the hybrid mode (electric heater enabled), the kiln-temperature profile was markedly different. Figure 3 presents the three days of the hybrid trial. Each morning at 09:00 the kiln (initially near ambient) was heated rapidly to the ~50 °C setpoint within 15–30 min, as the circulation fans distributed heat generated by the 2 kW heater. By approximately 09:30 the kiln air reached 50 °C and thereafter hovered close to this target for the remainder of the session. The controller cycled the heater on and off as needed to offset heat losses or dips in the solar input. Consequently, the kiln temperature was maintained at 50 °C from late morning to mid-afternoon. Minor fluctuations were observed: under strong sun the heater remained mostly off and the temperature occasionally nudged slightly above 50 °C; during overcast intervals the heater cycled more frequently, preventing significant temperature dips. In contrast to the solar-only mode, the hybrid kiln maintained the drying temperature much more consistently despite variable weather. Each day around 16:00 the trial ended, the heater was switched off and the kiln fans were shut down, causing a sharp temperature fall and equalisation with ambient conditions (visible as a steep drop at session end in Figure 3). These end-of-session drops highlight that stability was actively maintained only during operation.

With auxiliary heating, the kiln operated in a controlled manner similar to a conventional kiln. Throughout the 7-h drying period, the temperature rose for 50–90 min to reach 50 °C, depending on the intensity of solar irradiance, and remained at 50 ± 1 °C from 10:00 to 16:00. This demonstrates the effectiveness of the hybrid approach: the electric heater provided make-up heat whenever solar energy was insufficient, ensuring that the target temperature was met, while the heater output was naturally throttled down by the controller whenever solar gain was adequate.

3.5 Kiln-air equilibrium moisture content

Kiln-air EMC was computed throughout the day for both the non-heated and heated runs. Figure 4 shows the EMC curves from 09:00 to 16:00 for a representative day in each mode. In the morning, as the kiln warmed, EMC decreased rapidly. In the heated (hybrid) case, EMC decreased to approximately 2–3 % by mid-morning and remained very low and stable (≈ 2.5 % on average) for the rest of the day. By contrast, in the solar-only case EMC reached a minimum of approximately 5–7 % around noon (varying with each day's humidity conditions) and then drifted higher in the afternoon (often rising above 6 % by 16:00 as the kiln cooled slightly or drew in moister ambient air). Within-session variability was also greater without heating: pooled across the three solar-only days, the within-day SD of EMC was 1.4 %, compared with 0.3 % across the three hybrid days.

3.6 Energy consumption

One of the most significant advantages of the hybrid solar kiln is the reduction in external energy use. Heater on-time and the associated electrical energy were strongly correlated with daily irradiance. On a fully overcast day (heater running continuously from 09:00 to 16:00), the system would draw approximately 14.6 kWh over 7 h (mean draw 2.094 kW). This represents a worst-case theoretical baseline against which the SCF (Equation 4) is normalised; it does not represent the consumption of a real conventional kiln, which would itself cycle thermostatically. No fully overcast day was encountered during the trial.

During the actual hybrid trial days: on Day 1 (mixed sun and cloud) the heater was active for ~5.23 h of the 7-h session, drawing 11.0 kWh and giving an SCF of 25.2 %; on Day 2 (mostly sunny) heater run-time was 4.30 h, energy use 9.0 kWh, SCF 38.6 %; on Day 3 (clear sky, mid-session GHI ~890 W m^{-2}) heater run-time was only 1.45 h, energy use 3.0 kWh, SCF 79.3 %. These daily values should be read in the context of n = 3 days; longer monitoring across seasons is required before any annualised SCF can be claimed. Solar input therefore offset between one quarter and four fifths of the continuous-heating baseline across the three trial days. Even on the cloudiest trial day, solar gain displaced approximately one quarter of the maximum heater duty.

4. Discussion

These results are consistent with the expectations for a passive solar kiln. In moderate climates, solar kilns typically heat 10–30 °C above ambient, depending on insolation (Phonetip et al., 2022). The brief excursion to ~52 °C on Day 3 is consistent with prior reports of solar kilns reaching similar peak temperatures in clear weather; the inability to sustain it confirms the temperature-instability problem widely reported in the literature (Khouya, 2022; Lamrani et al., 2023; Ferrari et al., 2024) Such instability is widely associated with steep moisture gradients, internal drying stresses, and reduced quality in commercial timber drying; verifying these effects with the present prototype requires future trials with a wood load. Thus, while solar heating clearly raised the kiln's temperature well above ambient, it alone was insufficient to consistently maintain the optimal drying temperature of approximately 50 °C in this prototype. This finding reinforces the rationale for hybridising the system with supplemental heating.

Ambient temperature and GHI were the dominant predictors; ambient humidity contributed weakly. These findings align with those of Phonetip et al.,(2022) who showed that solar input drives morning thermal recharge while internal kiln RH substantially limits peak temperatures, decreasing by ~5 °C as the set RH rose from 20 % to 40 % and by a further ~5 °C from 40 % to 60 %.

In an exploratory refinement, including the kiln-air RH measured by the controller as an additional predictor raised the in-sample R^2 to ~0.97. Because kiln RH is itself downstream of kiln temperature, this refined model is endogenous and is reported here only to illustrate that humidity dynamics are the dominant residual source; it is not recommended for predictive use. Phonetip et al.(2018) previously demonstrated that solar-kiln temperature can be effectively modelled using thermal recharge–discharge curves, and Phonetip et al. (2019) subsequently validated the same model in an operating *Eucalyptus delegatensis* drying trial, achieving < 2 °C prediction error against measured kiln-air temperature. The regression developed in the present paper is intended as a coarser, climate-only counterpart to that validated dynamic model, suitable for site screening rather than for control. Together, these results suggest that simple reanalysis-driven regressions are adequate for pre-installation siting decisions, but that dynamic thermal–moisture models are required for control. Comparing the solar-only and hybrid results clearly highlights the benefits of the auxiliary heater. In passive mode, the kiln seldom reached 50 °C and could not hold it throughout the day; in hybrid mode ~50 °C was achieved every day by mid-morning and maintained for hours. From a processing perspective, this thermodynamic stability is the precondition for fast and uniform drying. The relationship between schedule stability and timber quality is, however, not monotonic: Langrish (2013) showed using a strain-based simulation of *Eucalyptus grandis* drying that gentler cyclic schedules can produce lower instantaneous strains than aggressive continuous schedules through mechanosorptive relaxation, and the intermittent solar-style schedules produced AS/NZS class-A quality in *E. delegatensis* (Phonetip, Ozarska, et al., 2019). Whether the present prototype, operated at a constant 50 °C, actually delivers faster and more uniform drying of timber must therefore be confirmed in a subsequent loaded trial in which moisture-gradient evolution and check formation can be measured directly. This observation echoes the findings of Ferrari et al.,(2024) who reported that their solar–biomass kiln could sustain higher drying temperatures and thereby reduce drying time and final moisture content relative to solar-alone drying.

This shows that auxiliary heat both raises kiln temperature and lowers kiln-air RH (since warmer air at the same absolute humidity has a lower saturation ratio), with ventilation removing moisture air from the chamber. The observed EMC of 2–3 % represents an exceptionally low value. Such low EMC values are at the lower limit of validity of the Hailwood–Horrobin sorption model and should be interpreted as indicating a strongly desiccating environment rather than as predictions of attainable wood moisture content. In practice, lumber drying is usually stopped long before such a low MC is reached (the typical final MC for many uses is 8–12 %); however, the low EMC implies a strong drying force (a large gradient between the wood's internal moisture and the air's capacity to take up water). In contrast, an EMC of 5–7 % (as in the solar-only kiln air) provides a smaller driving force. The hybrid kiln air was not only drier on average but also more constant in RH, which would help avoid surface re-moistening during humid intervals (Phonetip et al., 2018). The afternoon rise in EMC for the solar-only kiln implies that, as solar heating wanes, the chamber becomes progressively less effective at maintaining low humidity a hypothesis to be tested under load. These findings are consistent with previous observations on hybrid drying systems, where Ferrari et al.(Ferrari et al., 2024) reported that their hybrid solar kiln achieved a lower final wood moisture content than drying under ambient conditions.

Similarly, the much smaller variation in EMC observed with heating (only ± 0.3 % during steady operation) implies more uniform drying conditions, which is important for minimising drying stresses and defects. Overall, the hybrid system's ability to maintain EMC at approximately 2–3 % throughout the day is a clear advantage. It maximises the drying potential when wood moisture is high, and it can dry the air well below typical target MC levels, ensuring that even wet core sections of lumber would experience continuous drying pressure. In practice, a kiln operator might introduce steam or water spray at the end for conditioning if the EMC is too low (to avoid over-drying the wood surface). In summary, auxiliary heating lowered and stabilised kiln-air humidity, generating psychrometric conditions consistent with faster and more controlled drying; confirmation under load is left to future work.

This finding is broadly consistent with previous studies on the energy efficiency of solar-augmented drying. For instance, Khouya (2020) reported a ~50 % reduction in specific energy consumption (per unit wood dried) relative to a purely conventional process when thermal storage and heat recovery were integrated. Direct comparison must be made with care, however, because the two studies use different baselines: Khouya's 50 % is energy per dry mass against a conventional kiln, whereas this current paper 25–79 % is solar contribution against continuous heater operation. Even on the cloudiest trial day, the solar contribution was ~25 %; under Melbourne winter conditions, which are climatologically conservative compared with the tropical and sub-tropical sites where such systems are most likely to be deployed, an annualised SCF of 40–60 % is plausible but cannot be claimed without longer monitoring. This is a substantial reduction, underlining the economic and environmental advantage of the hybrid solar kiln. As Ferrari et al. (2024) highlighted, renewable heat sources can substantially lower drying costs (USD 0.009 kWh^{-1} for biomass furnace heat vs USD 0.14 kWh^{-1} for PV electricity in their case study). By maximising the use of "free" solar energy, the present system reduces reliance on grid electricity.

Comparison with prior hybrid solar kilns

To place the present results in context, Table 1 summarises kiln scale, climate, auxiliary configuration, control strategy, energy metric (and its baseline), and drying load for the most directly comparable studies in the recent literature. Two observations follow. First, all prior hybrid solar wood-kiln studies in this comparison were either simulated or operated at pilot scale (3–6 m^3 or larger); the present prototype is, to our knowledge, the smallest hybrid solar–electric wood kiln for which experimental SCF values have been reported. Second, the baselines against which "energy savings" are reported differ significantly between studies conventional kiln,(Ferrari et al., 2024; Khouya, 2020; Lamrani et al., 2021) solar-only, (Thomasson et al., 2024) continuous auxiliary heat, (Chi et al., 2022) or continuous-heater theoretical maximum (this work). This heterogeneity precludes a direct numerical comparison of savings percentages and supports the present reframing as a solar contribution fraction rather than a "saving".

The present study contributes the smallest, simplest, and most replicable end of this spectrum: a 0.94 m^3 chamber, a single 2 kW thermostatically controlled booster, and an empirical kiln-temperature regression driven by freely available reanalysis data. The methodology is therefore intended to lower the entry barrier to hybrid solar drying for smallholders and developing-country sawmills, complementing the more advanced control approaches reported at industrial scale (Chi et al., 2022; Lamrani et al., 2023).

5. Conclusion

Integrating solar heating with an auxiliary electric heater can effectively maintain drying temperatures around 50 °C even under fluctuating weather conditions. Without auxiliary heat, kiln temperature varied with sunlight (peaking ~40–52 °C on the sunniest day but lower on cloudier days), and kiln-air EMC was 5–7 %, indicating limited drying potential. With electric heater support the kiln achieved a stable 50 ± 1 °C environment with kiln-air EMC of 2–3 %, generating psychrometric conditions consistent with rapid drying. Whether these psychrometric conditions translate to measurable improvements in drying rate, moisture-gradient uniformity, and timber quality must be confirmed under load.

A simple linear model reasonably predicted kiln temperature from ambient reanalysis-based weather data (training $R^2 = 0.70$). The model is suitable for first-order site screening before installation; finer control will require dynamic thermal–moisture modelling.

The hybrid kiln consumed substantially less electrical energy than a continuously running 2 kW heater would, with a solar contribution fraction of 25–79 % across the three trial days.

This study has four explicit limitations that should be addressed before generalising the findings: (i) only three days of trials per mode; (ii) ambient meteorological data obtained from reanalysis rather than on-site sensors; (iii) operation in a single winter season at a single temperate site; and (iv) the absence of a wood load, which means that all drying-rate and product-quality implications remain hypotheses.

6. Conflict of Interest

The authors declare that no conflict of interest with any financial organization regarding the material discussed in the manuscript. During the preparation of this work the authors used ChatGPT and Claude AI to expand literature searches and to improve grammar, clarity, and quality of written communication. After using these tools, the authors reviewed and edited the content and take full responsibility for the content of the publication.

7. Acknowledgements

The first author gratefully acknowledges the International Education Innovation Fund (IEIF-ASEAN) for providing financial support for his postdoctoral research, and the technical support from the project "Sustainable Expansion of Forestry and Wood Processing in Laos and Australia" (Project No. FST/2023/153) during the trials conducted at the University of Melbourne, Australia. The authors also thank Mr Phouthavanh Bounyasane for his assistance during the installation of the solar-kiln prototype.

8. References

Bux, M., Bauer, K., Mühlbauer, W., & Conrad, T. (2001). Solar-assisted drying of timber at industrial scale. *Southern African Forestry Journal*, *192*, 73–78. https://doi.org/10.1080/20702620.2001.10434136

Chi, X., Tang, S., Du, X., Liu, Y., Zhang, W., & Cheng, W. (2022). Effects of air-assisted solar drying on poplar lumber drying processes in sub frigid zone regions. *Drying Technology*, *40*(16), 3580–3590. https://doi.org/10.1080/07373937.2022.2068571

Chtioui, S., & Khouya, A. (2024). Optimizing solar energy for wood drying under various climates: A comparative study of flat plate and photovoltaic thermal solar collectors. *Renewable Energy*, *221*, 119691. https://doi.org/10.1016/j.renene.2023.119691

Copernicus Atmosphere Monitoring Service. (2025). *CAMS solar radiation time-series* [Dataset]. Copernicus Atmosphere Monitoring Service. https://ads.atmosphere.copernicus.eu/datasets/cams-solar-radiation-timeseries

Copernicus Climate Change Service. (2025). *CERRA sub-daily regional reanalysis data for Europe on single levels from 1984 to present* [Dataset]. Copernicus Climate Change Service Climate Data Store. https://doi.org/10.24381/CDS.622A565A

De Vore, J. B., Denny, G. S., & Harper, T. S. (1999). A commercially viable solar wood drying kiln system. *Drying Technology*, *17*(1–2), 137–154. https://doi.org/10.1080/07373939908917529

Ferrari, S., Cuccui, I., Cerutti, P. O., & Allegretti, O. (2024). A hybrid solar/biomass active indirect kiln dryer for timber in the Democratic Republic of Congo. *International Journal of Ambient Energy*, *45*(1), 2367109. https://doi.org/10.1080/01430750.2024.2367109

Glass, S. V., & Zelinka, S. L. (2010). Moisture relations and physical properties of wood. In *Wood Handbook: Wood as an Engineering Material* (pp. 4–1). U.S. Department of Agriculture, Forest Service, Forest Products Laboratory.

Helwa, N. H., Khater, H. A., Enayet, M. M., & Hashish, M. I. (2004). Experimental evaluation of solar kiln for drying wood. *Drying Technology*, *22*(4), 703–717. https://doi.org/10.1081/DRT-120034258

Khater, G., Bahnasawy, H., Oraiath, T., Alhag, K., Shuraym, A., Moustapha, E., Elwakeel, E., Elbeltagi, A., Salem, A., Metwally, A., Abdalla, I., Hussein, M., Abdeen, A., Hussein, M., & Abdeen, I. (2024). Assessment of a LPG hybrid solar dryer assisted with smart air circulation system for drying basil leaves. *Scientific Reports*, *14*(1), 23922. https://doi.org/10.1038/s41598-024-74751-4

Khater, H. A., Helwa, N. H., Enayet, M. M., & Hashish, M. I. (2004). Optimization of solar kiln for drying wood. *Drying Technology*, *22*(4), 677–701. https://doi.org/10.1081/DRT-120034254

Khouya, A. (2020). Effect of regeneration heat and energy storage on thermal drying performance in a hardwood solar kiln. *Renewable Energy*, *155*, 783–799. https://doi.org/10.1016/j.renene.2020.03.178

Khouya, A. (2022). Energy analysis of a combined solar wood drying system. *Solar Energy*, *231*, 270–282. https://doi.org/10.1016/j.solener.2021.11.068

Kong, D., Wang, Y., Li, M., & Liang, J. (2024). A comprehensive review of hybrid solar dryers integrated with auxiliary energy and units for agricultural products. *Energy*, *293*, 130640. https://doi.org/10.1016/j.energy.2024.130640

Lamrani, B., Bekkioui, N., & Draoui, A. (2020). Modelling and simulation of a hybrid solar-electrical dryer of wood integrated with latent heat thermal energy storage system. *Thermal Science and Engineering*

Progress, *18*, 100545. https://doi.org/10.1016/j.tsep.2020.100545

Lamrani, B., Bekkioui, N., & Draoui, A. (2021). Energy analysis and economic feasibility of wood dryers integrated with heat recovery unit and solar air heaters in cold and hot climates. *Energy*, *228*, 120511. https://doi.org/10.1016/j.energy.2021.120511

Lamrani, B., Bekkioui, N., Simo-Tagne, M., & Ndukwu, M. C. (2023). Recent progress in solar wood drying: An updated review. *Drying Technology*, *41*(5), 605–627. https://doi.org/10.1080/07373937.2022.2112048

Langrish, T. A. G. (2013). Comparing continuous and cyclic drying schedules for processing hardwood timber: The importance of mechanosorptive strain. *Drying Technology*, *31*(10), 1091–1098. https://doi.org/10.1080/07373937.2013.769449

Monesh, S., Shankar, A., Ezhilarasan, S., Tiwari, S., Sahdev, R. K., & Tiwari, P. (2024). Comparison of different solar dryers with and without heat storage for crop drying: A review. *Environmental Progress & Sustainable Energy*, *43*(6), e14490. https://doi.org/10.1002/ep.14490

Phonetip, K., Brodie, G. I., Ozarska, B., & Belleville, B. (2018). Simulating solar kiln conditions using a conventional kiln. *BioResources*, *13*(2), 3740–3752. https://doi.org/10.15376/biores.13.2.3740-3752

Phonetip, K., Brodie, G. I., Ozarska, B., & Belleville, B. (2019). Drying timber in a solar kiln using an intermittent drying schedule of conventional laboratory kiln. *Drying Technology*, *37*(10), 1300–1312. https://doi.org/10.1080/07373937.2018.1496337

Phonetip, K., Brodie, G., & Smith, H. (2022). Effect of solar insolation on a solar kiln performance. *Souphanouvong University Journal of Multidisciplinary Research and Development*, *8*(1), 125–135.

Phonetip, K., Ozarska, B., Belleville, B., & Brodie, G. I. (2019). Comparing two intermittent drying schedules for timber drying quality. *Drying Technology*, *37*(2), 220–228. https://doi.org/10.1080/07373937.2018.1445638

Simo-Tagne, M., & Ndi-Azese, M. (2021). Thermal, economic, and environmental analysis of a novel solar dryer for firewood in various temperate and tropical climates. *Solar Energy*, *225*, 1072–1087. https://doi.org/10.1016/j.solener.2021.07.046

Simo-Tagne, M., Ndukwu, M. C., & Azese, M. N. (2020). Experimental modelling of a solar dryer for wood fuel in Épinal (France). *Modelling*, *1*(1), 39–52. https://doi.org/10.3390/modelling1010003

Stéphan, A., Sauceau, M., Lecomte, D., & Bahloul, R. (2025). A model-based advanced control system to cope with energy fluctuations in industrial wood drying. *Drying Technology*. https://doi.org/10.1080/07373937.2025.2456789

Thomasson, T., Kiviranta, K., Tähtinen, M., & Tuomaala, M. (2024). Experimental and techno-economic analysis of solar-assisted heat pump drying of biomass. *Energy Reports*, *12*, 1428–1443. https://doi.org/10.1016/j.egyr.2024.07.018

Udomkun, P., Romuli, S., Schock, S., Mahayothee, B., Sartas, M., Wossen, T., Njukwe, E., Vanlauwe, B., & Müller, J. (2020). Review of solar dryers for agricultural products in Asia and Africa: An innovation landscape approach. *Journal of Environmental Management*, *268*, 110730. https://doi.org/10.1016/j.jenvman.2020.110730

Nomenclature

Symbol	Description	Unit
E_{fans}	Energy consumption of circulation fans	Wh
E_{total}	Total nominal energy consumption (fans + heater × t)	Wh
E_{rt}	Real-time energy consumption from logged heater on-time	Wh
P_{fans}	Total rated power of circulation fans	W
P_{heater}	Rated power of electric booster heater	W
T_a	Ambient air temperature	°C
T_{kiln}	Kiln-air temperature	°C
P_{kt}	Regression-predicted kiln-air temperature	°C
RH_a	Ambient relative humidity	%
RH_{kiln}	Kiln-air relative humidity	%
GHI	Global horizontal irradiance at the surface	$W\ m^{-2}$
SCF	Solar contribution fraction	%
EMC	Equilibrium moisture content of kiln air	%
t	Session time	h
t_{on}	Cumulative heater on-time over a session	h
R^2	Coefficient of determination	

Abbreviations: CAMS, Copernicus Atmosphere Monitoring Service; CERRA, Copernicus European Regional Reanalysis; MC, moisture content; PCM, phase-change material; PV/T, photovoltaic/thermal; PWM, pulse-width modulation; SD, standard deviation.

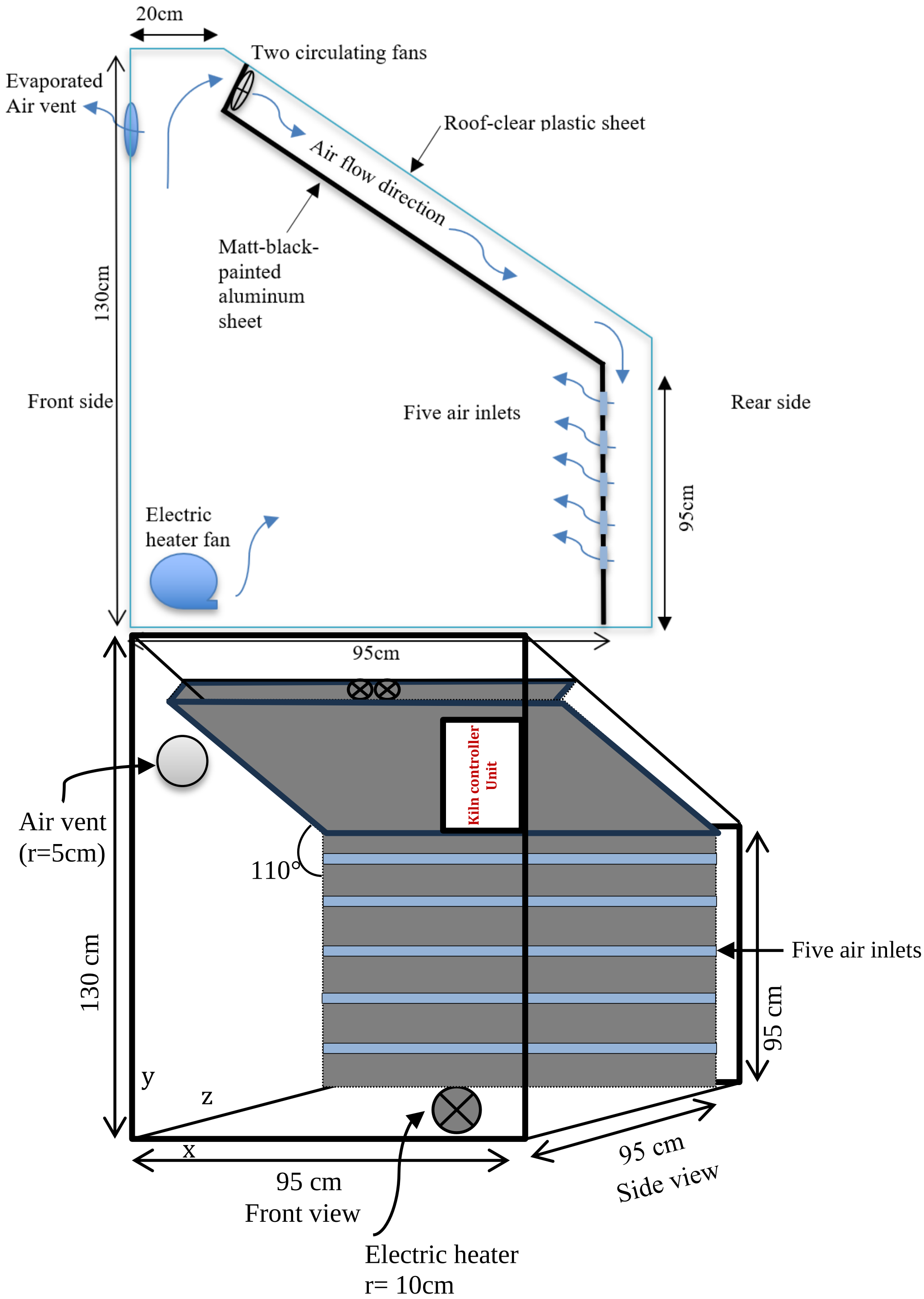

Figure 1. Schematic of the 0.94 m³ prototype hybrid solar–electric kiln used in this study. The side view (a) and the isometric view (b).

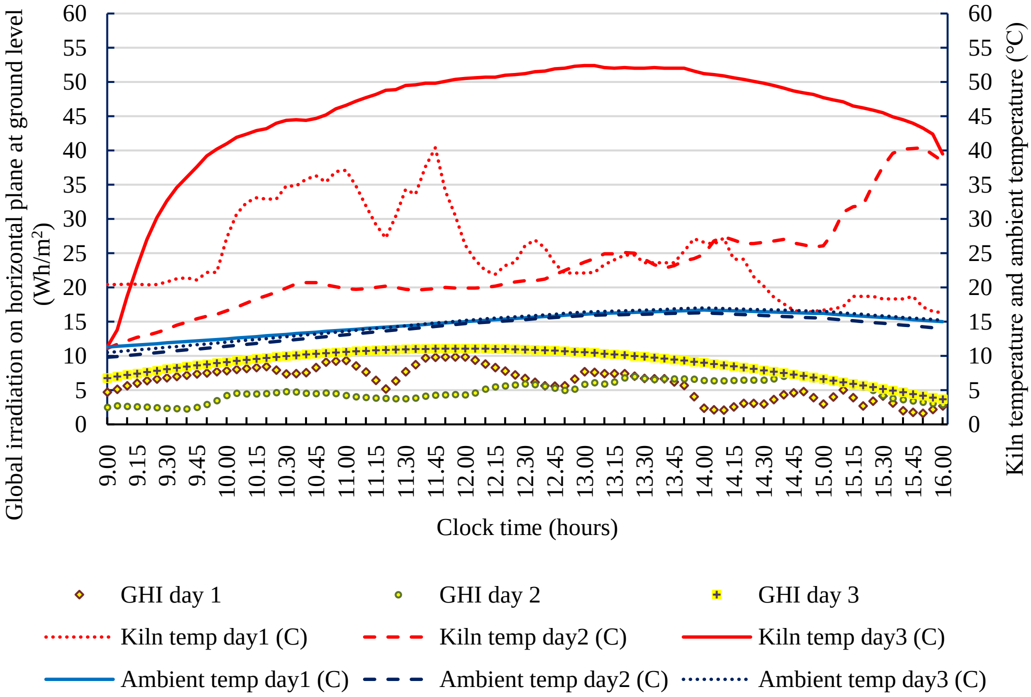

Figure 2. Time series of kiln air temperature (dashed black), ambient air temperature (dotted grey), the 50 °C setpoint (solid red), and global horizontal irradiance (grey filled area; right axis, W m⁻²) during three solar-only trials (Days 1–3) at Bundoora, Victoria, Australia (37.83° S, 145.02° E), 09:00–16:00 local time, July–August 2025. The kiln exceeded 50 °C only briefly on Day 3, the day of highest irradiance. Each trial day is presented as a separate panel.

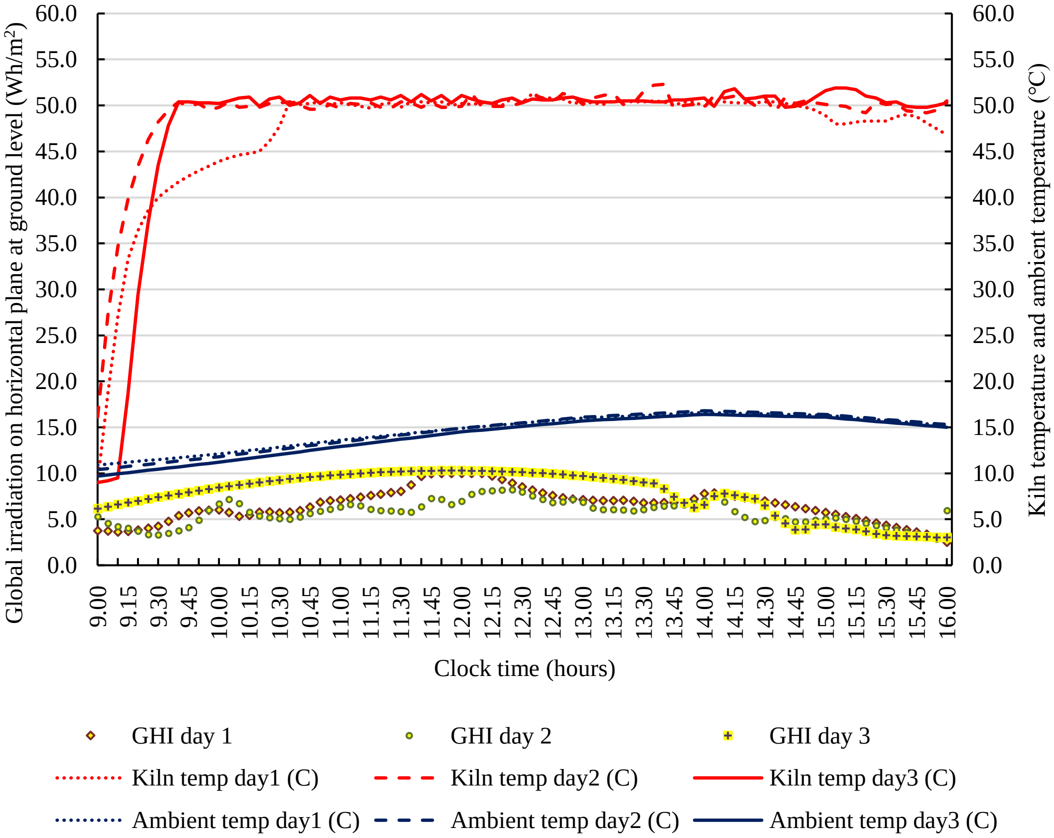

Figure 3. Time series of kiln air temperature (dashed black), ambient air temperature (dotted grey), the 50 °C setpoint (solid red), and global horizontal irradiance (grey filled area; right axis, W m⁻²) during three hybrid trials (Days 1–3) with

the 2 kW electric fan-heater enabled. The kiln reached the 50 °C setpoint within 15–30 min of start-up and was maintained at 50 ± 1 °C until shutdown at 16:00. Each trial day is presented as a separate panel.

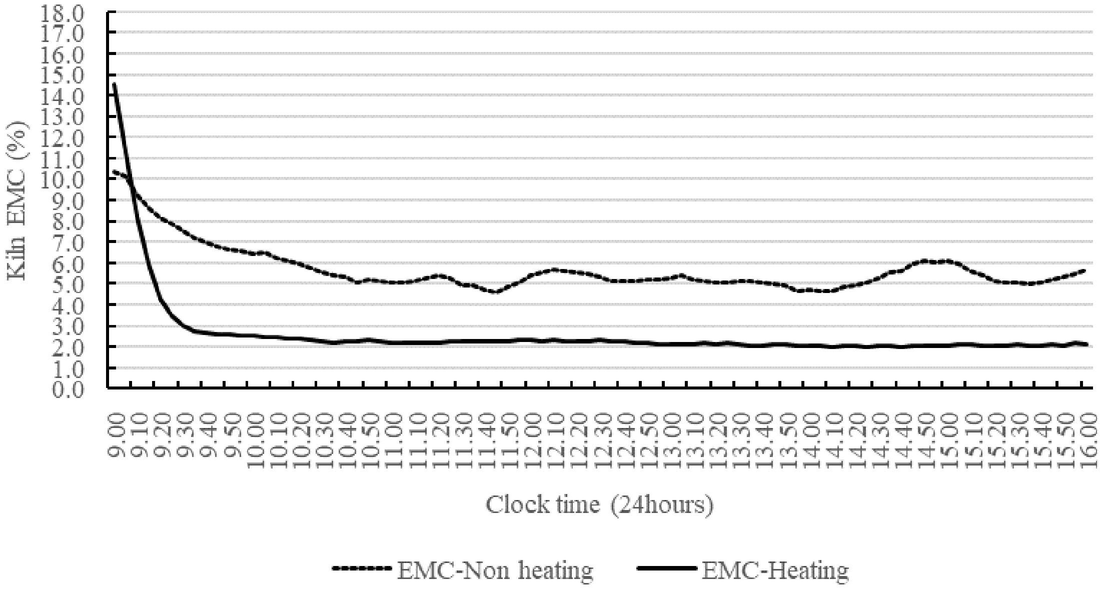

Figure 4. Kiln-air equilibrium moisture content (EMC) versus time of day, 09:00–16:00, for a representative day under solar-only operation (open symbols) and a representative day under hybrid operation with the 2 kW electric fan-heater (closed symbols). EMC was computed from the kiln-air temperature and the controller-measured kiln RH using the Hailwood–Horrobin sorption model (Glass and Zelinka 2010). Shaded bands indicate ±1 standard deviation across the three trial days in each mode.

Table 1. Comparison of the present prototype with recent hybrid solar wood-drying studies.

Study	**Scale**	**Climate**	**Auxiliary**	**Control**	**Energy metric (baseline)**	**Load**
This study	0.94 m³	Melbourne winter, temperate	2 kW electric fan-heater	Thermostat (± 1 °C)	SCF 25–79 % (vs continuous heater, 3 days)	Empty kiln
(Ferrari et al., 2024)	~6 m³	DRC, tropical	Biomass furnace + PV	Industrial	0.4–1.4 % MC day⁻¹ (vs solar alone)	Sawn timber
(Khouya, 2020)	Simulation	Mediterranean	Regeneration heat + storage	Model-based	~50 % reduction (vs conventional)	Hardwood (sim.)
(Lamrani et al., 2020)	Simulation	Tangier, Morocco	Electric heater + PCM	Simulation	Continuous drying enabled (vs solar)	Wood boards (sim.)
(Lamrani et al., 2021)	Simulation	Cold + hot climates	PV/T + heat recovery	Simulation	49.5–67.5 % annual reduction (vs conventional)	Wood (sim.)
(Chi et al., 2022)	Field	NE China, sub-frigid	Air-energy (HP)	Intermittent vs continuous	50.7 % electrical-energy improvement (vs continuous AE)	Poplar lumber
(Thomasson et al., 2024)	Pilot	Finland, cold	Solar thermal + air-source HP	Optimised	+45 % specific electricity; 3× drying rate (vs solar)	Woody biomass